

*Supplement of*

**Evolution of OH reactivity in low-NO volatile organic compound oxidation investigated by  
the fully explicit GECKO-A model**

Zhe Peng<sup>1</sup>, Julia Lee-Taylor<sup>1,2</sup>, Harald Stark<sup>1,3</sup>, John J. Orlando<sup>2</sup>, Bernard Aumont<sup>4</sup> and Jose L. Jimenez<sup>1</sup>

<sup>1</sup> Cooperative Institute for Research in Environmental Sciences and Department of Chemistry,  
University of Colorado, Boulder, Colorado 80309, USA

<sup>2</sup> Atmospheric Chemistry Observation and Modeling Laboratory, National Center for Atmospheric  
Research, Boulder, Colorado 80307, USA

<sup>3</sup> Aerodyne Research Inc., Billerica, Massachusetts 01821, USA

<sup>4</sup> Laboratoire Inter-Universitaire des Systèmes Atmosphériques (LISA), UMR 7583, Université Paris-Est  
Créteil, Université de Paris, CNRS, Institut Pierre Simon Laplace, 94010 Créteil, France

Correspondence: Zhe Peng ([zhe.peng@colorado.edu](mailto:zhe.peng@colorado.edu)) and Jose L. Jimenez  
([jose.jimenez@colorado.edu](mailto:jose.jimenez@colorado.edu))

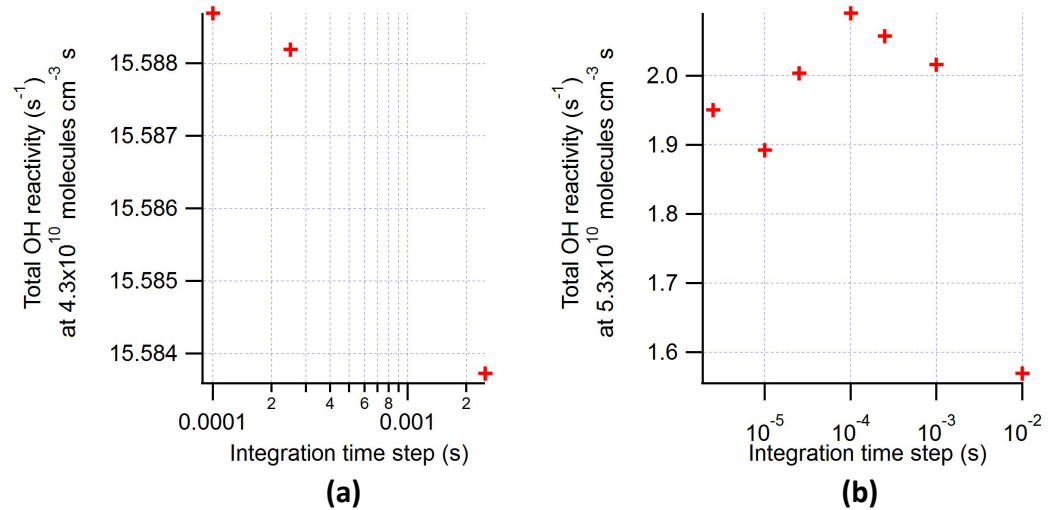


**Figure S1.** Total OH reactivity (OHR) of organics at OH exposure of (a)  $4.3 \times 10^{10}$  ad (b)  $5.3 \times 10^{10}$  molecules  $\text{cm}^{-3} \text{s}$  as a function of integration timestep in the test simulations for the (a) m-xylene and (b) isoprene oxidation flow reactor (OFR) cases at relative humidity of 70%, high lamp setting, and initial OHR of  $10 \text{ s}^{-1}$ . Note that the mechanisms in these test simulations are similar but not exactly the same as in the corresponding model cases shown in Table 1.

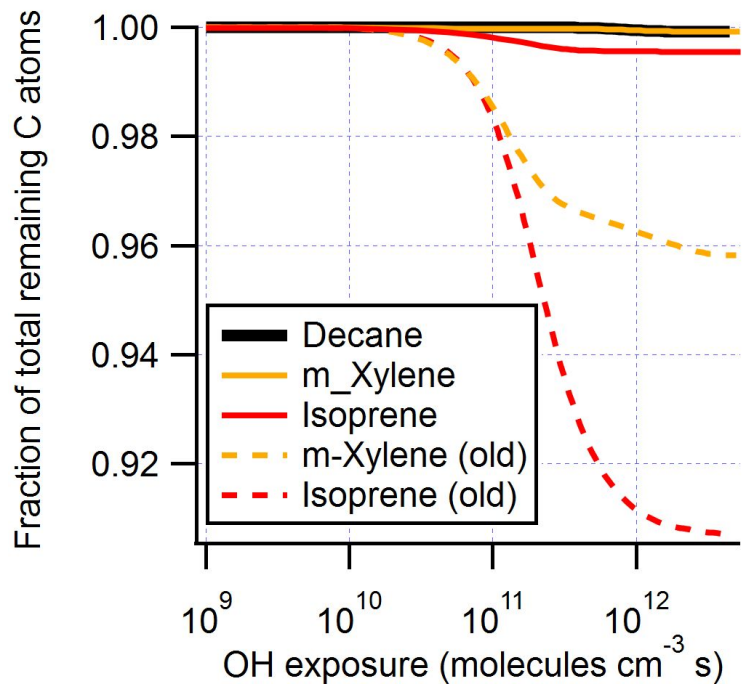


**Figure S2.** Fractions of total remaining C atoms as a function of OH exposure in the ambient cases with constant sunlight of the photooxidations of decane, m-xylene, and isoprene. Also shown for comparison are the simulations for m-xylene and isoprene with the old mechanisms whose problem of non-conservation of C atoms in some reactions has not been fixed.

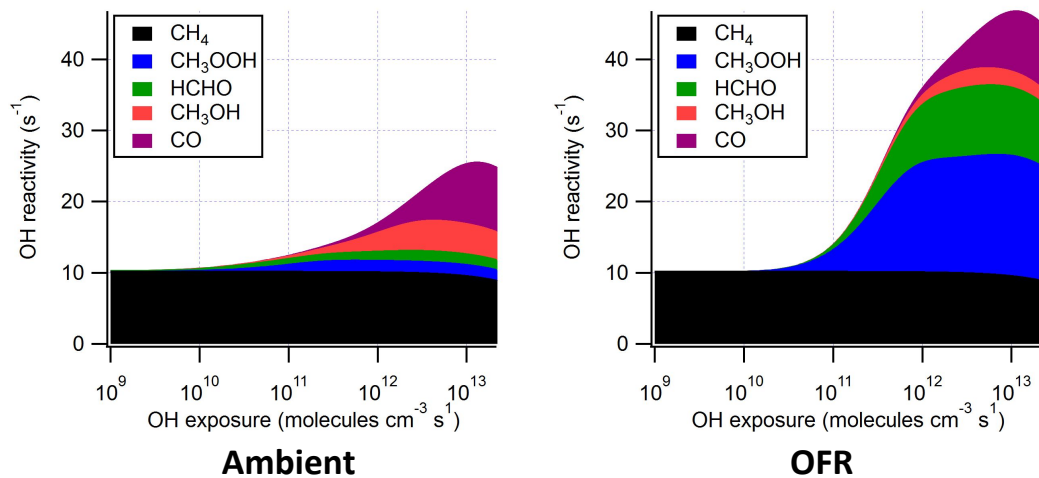


**Figure S3.** OH reactivity (OHR) of the organics as a function of OH exposure in the ambient case with constant sunlight; and in the OFR case at relative humidity of 70% and high lamp setting, both with initial OHR of  $10 \text{ s}^{-1}$  of methane photooxidation.

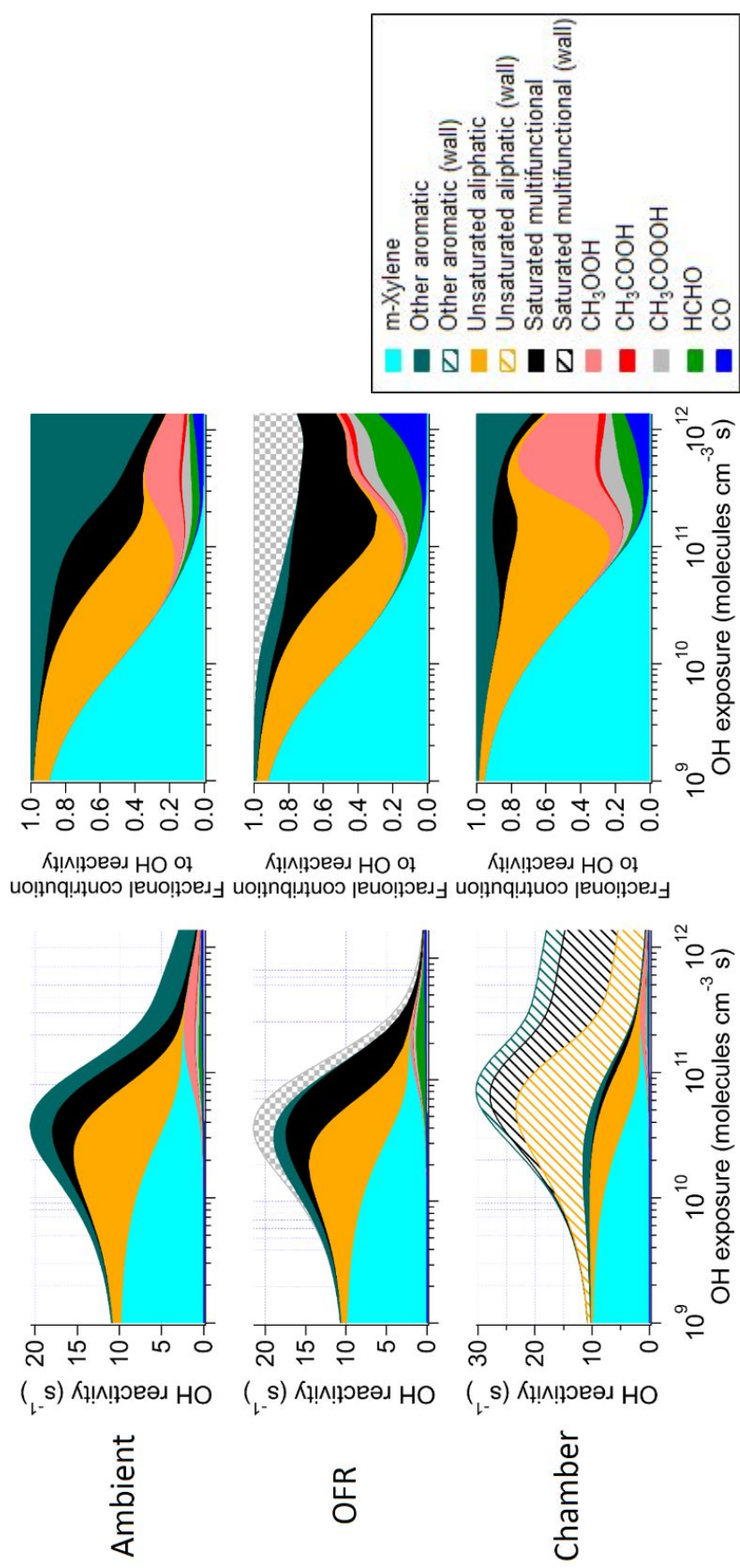


**Figure S4.** Same format as Fig. 4, but for m-xylene photooxidation.

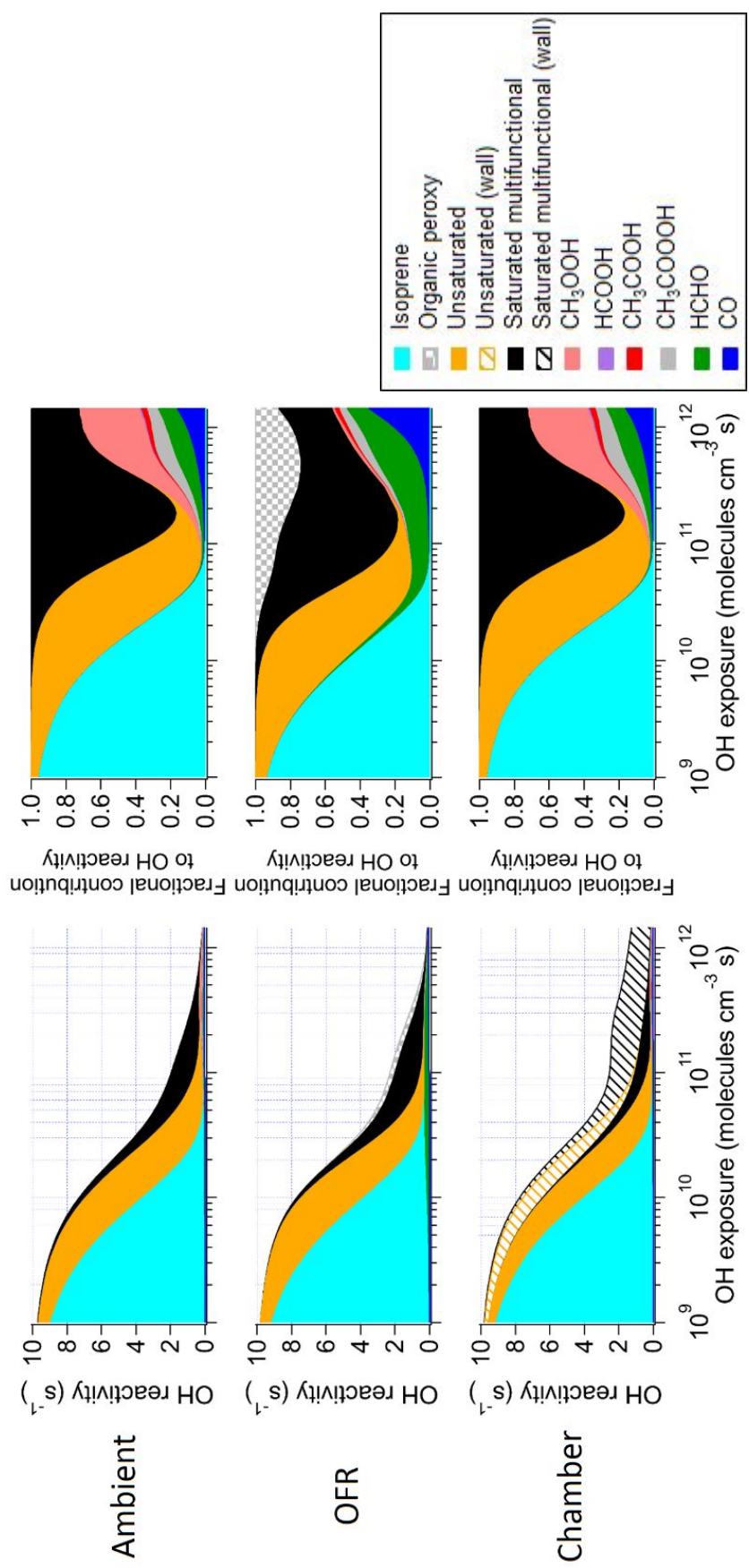
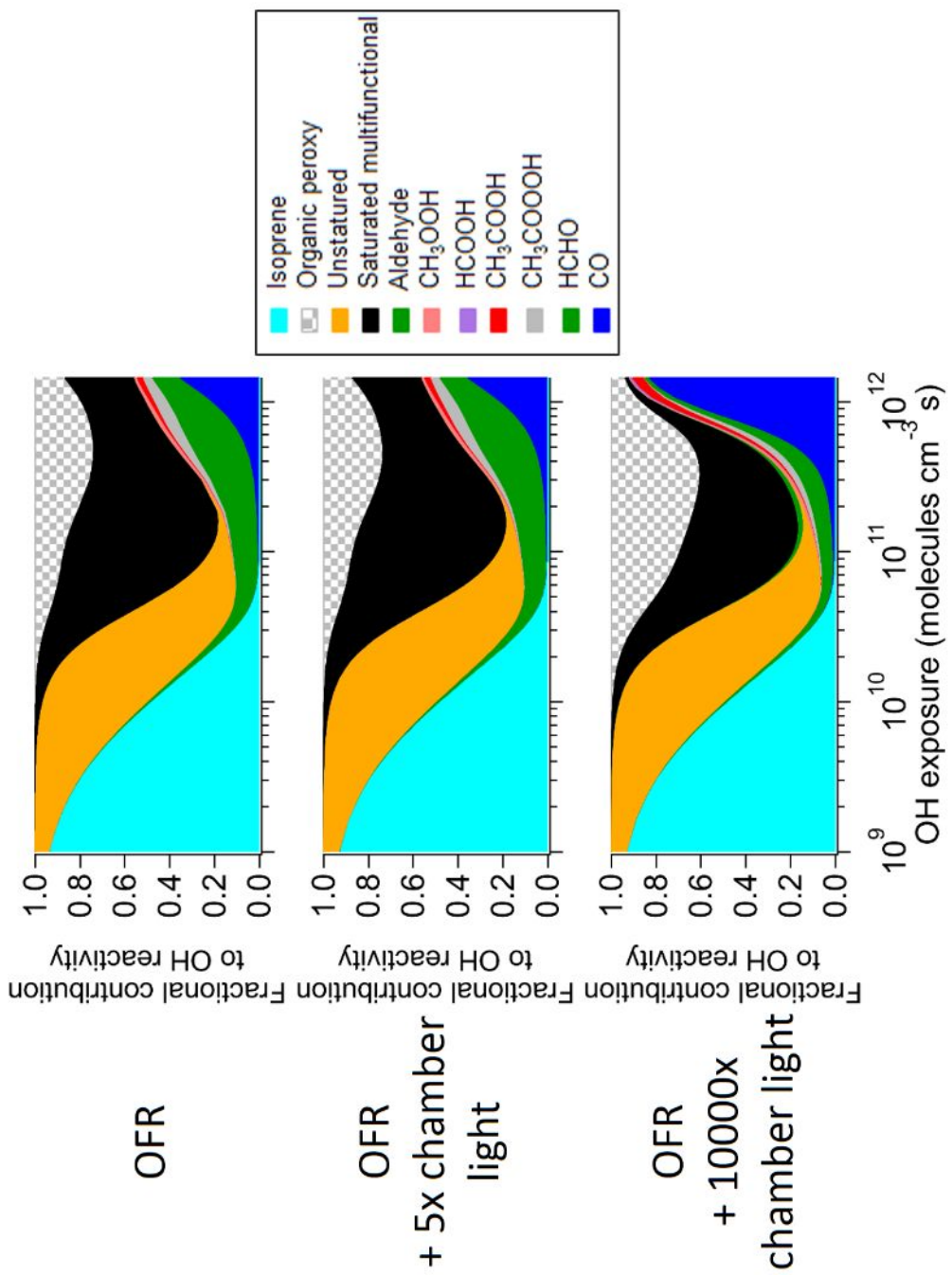
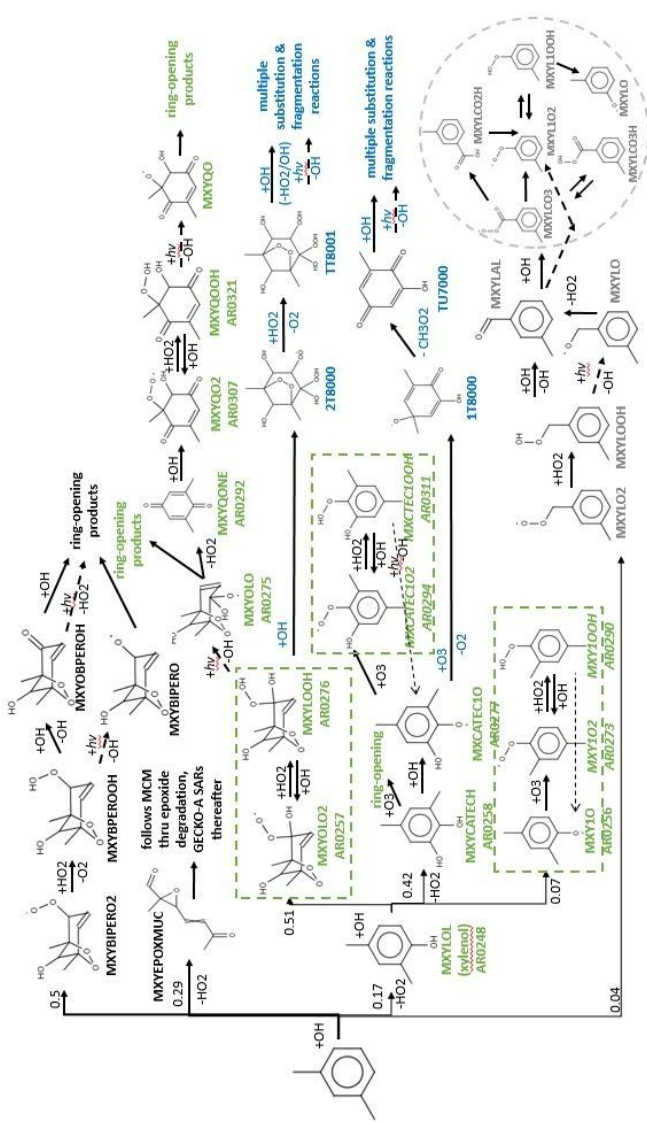


Figure 5. Same format as Fig. 4, but for isoprene photooxidation.



**Figure S6.** Fractional contributions of the main species and types of species to the organic OHR as a function of OH exposure in the standard OFR case of isoprene photooxidation with relative humidity of 30%, medium UV lamp setting, and two sensitivity cases based on this OFR case, with additional UV irradiation corresponding to 5 and 10000 times the UV source of the University of Colorado Environmental Chamber Facility, respectively. The types of species shown in this figure exclude the C1 and C2 species listed separately.

**Scheme S1.** Mechanism of m-xylene photooxidation in the absence of NO<sub>x</sub>, derived from MCM v3.2 (Jenkin et al., 2003; Bloss et al., 2005). Numbers refer to branching ratios. Photolysis pathways (which are usually minor) are indicated with dashed arrows. Xylenol oxidation pathways and products are shown with green (MCM v 3.2) or blue text (pathways and products added in this study). Species that persist anomalously under low-NO<sub>x</sub> conditions are indicated with dashed borders. Pathways ending in text (e.g. “ring-opening products”) progress within GECKO-A to complete oxidation. Figure adapted from MCM website, <http://mcm.leeds.ac.uk/MCMv3.3.1>, accessed July 3, 2020.



**Scheme S2.** Mechanism of methane photooxidation. Numbers refer to branching ratios.

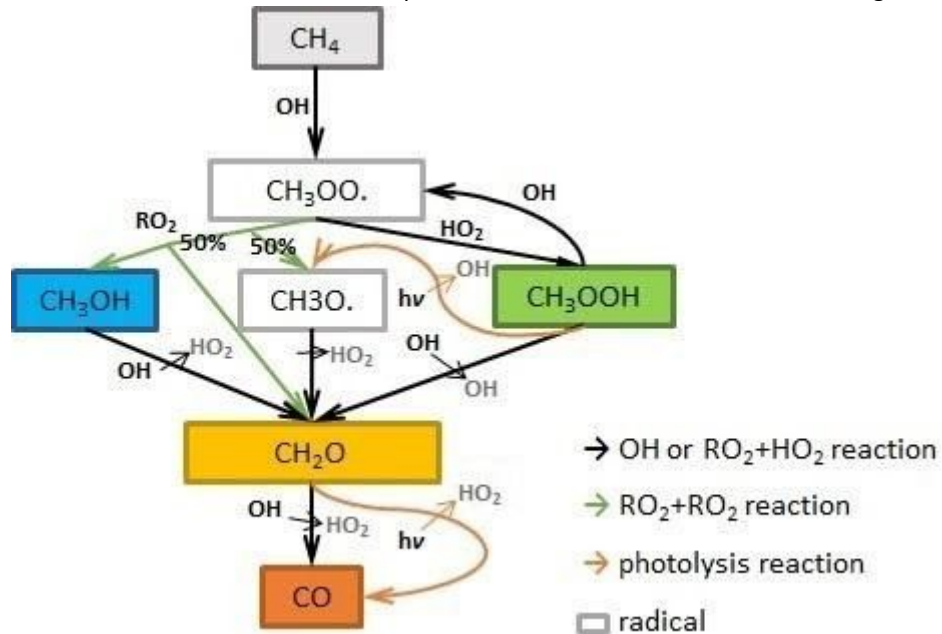


**Table S1.** Extension of reference absorption cross-sections ( $\sigma$ ) and branching ratios ( $\phi$ ) of organic photolysis to 185 nm and 254 nm

Species, channel	$\sigma_{185\text{nm}}$	$\Phi_{185\text{nm}}$ (if $\neq 1$ )
$\text{CH}_2\text{O}$	$3.64 \times 10^{-18}$ Cooper (1996) 184 nm	
$\rightarrow \text{H}_2 + \text{CO}$		0.44 Formula extrapolation, Röth (2015)
$\rightarrow \text{HCO} + \text{H}$		0.56 Formula extrapolation, Röth (2015)
$\text{CH}_3\text{OOH}$	$9.0 \times 10^{-19}$ rough extrapolation from 210-280nm data <sup>a</sup>	
$\text{CH}_2(\text{OH})\text{OOH}$	$9.0 \times 10^{-19}$ estimate after $\text{CH}_3\text{OOH}$	
$\text{CH}_3\text{CHO}$	$7.84 \times 10^{-20}$ <sup>a</sup>	
$\text{CHOCHO}$	$4.80 \times 10^{-19}$ Zhu (1996) at 193nm	
$\rightarrow \text{H}_2 + 2 \text{ CO}$		0.81 data extrapolation <sup>b</sup> (225nm)
$\rightarrow 2 \text{ CHO}$		0.16 data extrapolation <sup>b</sup> (225nm)
$\rightarrow \text{CH}_4 + \text{CO}$		0.03 data extrapolation <sup>b</sup> (225nm)
$\text{CH}_2(\text{OH})\text{CHO}$	$3.85 \times 10^{-18}$ Karandunandan (2007) at 184.9nm	
$\text{CH}(\text{O})\text{C}(\text{O})\text{OH}$	$4.0 \times 10^{-19}$ rough extrapolation from Back & Yamamoto (1985) (200nm)	
$\rightarrow \text{HCHO} + \text{CO}_2$		0.84
$\rightarrow \text{HCO} + 2 \text{ CO}$		0.16
$\text{C}(\text{O})(\text{OH})\text{C}(\text{O})\text{OH}$	$1.0 \times 10^{-18}$ estimate after $\text{CH}(\text{O})\text{C}(\text{O})\text{OH}$ and $\text{CH}_3\text{C}(\text{O})\text{C}(\text{O})\text{OH}$	
$\rightarrow \text{HC}(\text{O})\text{OH} + \text{CO}_2$		0.72 Yamamoto (1985) (255-309 nm)
$\rightarrow \text{HC}(\text{O})\text{OH} + \text{CO}_2$		0.27 Yamamoto (1985) (255-309 nm)
$\text{CH}_3\text{CH}_2\text{CHO}$	$1.43 \times 10^{-17}$ Lucaleau & Sandorfy (1970) (184.8 nm)	
$\text{CH}_3\text{COCH}_3$	$2.96 \times 10^{-18}$ Gierczak (2003) (184.9 nm, 242 K) [note: 296K value is $3.01 \times 10^{-18}$ ]	
$\text{CH}_3\text{CHOCHO}$	$3.71 \times 10^{-18}$ data extrapolation <sup>b</sup> (200-215 nm)	
$\rightarrow \text{CH}_3\text{C}(\cdot)\text{O} + \text{CHO}$		0.90 Raber (1995) (220-320 nm)
$\rightarrow \text{CH}_3\text{CHO} + \text{CO}$		0.05 Raber (1995) (220-320 nm)
$\rightarrow \text{CH}_4 + 2 \text{ CO}$		0.05 Raber (1995) (220-320 nm)
$\text{CH}_3\text{COCH}_2\text{OH}$	$5.40 \times 10^{-18}$ Dillon (2006) (184.9 nm)	
$\text{CH}_3\text{C}(\text{O})\text{C}(\text{O})\text{OH}$	$1.0 \times 10^{-17}$ rough extrapolation from JPL 10-6 (252-280 nm)	
		0.37 Moortgat (1999) (251-400 nm)

Species, channel	$\sigma_{254\text{nm}}$	$\Phi_{254\text{nm}}$
$\text{CHOCHO}$	$1.60 \times 10^{-20}$ Volkamer (2005) at 254nm	
$\rightarrow \text{H}_2 + 2 \text{ CO}$		0.54 data interpolation <sup>b</sup>
$\rightarrow 2 \text{ CHO}$		0.16 data interpolation <sup>b</sup>
$\rightarrow \text{CH}_4 + \text{CO}$		0.32 data interpolation <sup>b</sup>
$\text{C}(\text{O})(\text{OH})\text{C}(\text{O})\text{OH}$	$6.55 \times 10^{-20}$ extrapolation from Yamamoto (1985) (255-260 nm)	
$\rightarrow \text{HC}(\text{O})\text{OH} + \text{CO}_2$		0.72 Yamamoto (1985) (255-309 nm)
$\rightarrow \text{CO}_2 + \text{CO} + \text{H}_2\text{O}$		0.27 Yamamoto (1985) (255 -309 nm)

<sup>a</sup> Data from online spectral atlas: Keller-Rudek, H., Moortgat, G. K., Sander, R., and Sørensen, R., The MPI-Mainz UV/VIS spectral atlas of gaseous molecules of atmospheric interest, Earth Syst. Sci. Data, 5, 365–373, (2013)

<sup>b</sup> Data from JPL 10-6 (Sander et al, 2011)

## References:

- Back, R.A. and S. Yamamoto, "The gas-phase photochemistry and thermal decomposition of glyoxylic acid," *Can. J. Chem.* 63, 542-548, doi: 10.1021/j100250a014, 1985.
- Cooper, G., J.E. Anderson, and C.E. Brion, "Absolute photoabsorption and photoionization of formaldehyde in the VUV and soft X-ray regions (3-200 eV)," *Chem. Phys.* 209, 61-77, doi: 10.1016/0301-0104(96)00079-1, 1996.
- Dillon, T.J., A. Horowitz, D. Hölscher, J.N. Crowley, L. Vereecken, and J. Peeters, "Reaction of HO with hydroxyacetone ( $\text{HOCH}_2\text{C}(\text{O})\text{CH}_3$ ): rate coefficients (233-363 K) and mechanism," *Phys. Chem. Chem. Phys.* 8, 236-246, doi: 10.1039/B513056E, 2006.
- Gierczak, T., M.K. Gilles, S. Bauerle, and A.R. Ravishankara, "Reaction of hydroxyl radical with acetone. 1. Kinetics of the reactions of OH, OD, and  $^{18}\text{OH}$  with acetone and acetone-d<sub>6</sub>," *J. Phys. Chem. A* 107, 5014-5020, doi: 10.1021/jp027301a, 2003.
- Karunandan, R., D. Hölscher, T.J. Dillon, A. Horowitz, and J.N. Crowley, Reaction of HO with glycolaldehyde,  $\text{HOCH}_2\text{CHO}$ : Rate coefficients (240-362 K) and mechanism, *J. Phys. Chem. A* 111, 897-908, doi: 10.1021/jp0649504, 2007.
- Keller-Rudek, H., Moortgat, G. K., Sander, R., and Sørensen, R. The MPI-Mainz UV/VIS spectral atlas of gaseous molecules of atmospheric interest, *Earth Syst. Sci. Data*, 5, 365-373, doi:10.5194/essd-5-365-2013, 2013.
- Lee, A.M.D., J.D. Coe, S. Ullrich, M.L. Ho, S.-J. Lee, B.-M. Cheng, M.Z. Zgierski, I-C. Chen, T.J. Martinez, and A. Stolow, Substituent effects on dynamics at conical intersections:  $\alpha,\beta$ -enones, *J. Phys. Chem. A* 111, 11948-11960, doi: 10.1021/jp074622j, 2007.
- Lucazeau, G., and C. Sandorfy, On the far-ultraviolet spectra of some simple aldehydes, *J. Mol. Spectrosc.* 35, 214-231, doi: 10.1016/0022-2852(70)90199-2, 1970.
- Moortgat, G., Wirtz, K., Pons, N., Jensen, N., Horth, J., Winterhalter, R., Ruppert, L., Magneron, L., Tadic, J., and Mellouki, A.: Trends in tropospheric photodissociation rates of selected carbonyl compounds, in: Proceedings of the EC/Eurotrac-2 joint workshop, edited by: Vogt, R. and Axelsdottir, G., 28-31, ISBN 3-00-005414-6, Aachen, 1999.
- Orlando, J.J., G.S. Tyndall, J.-M. Fracheboud, E.G. Estupiñan, S. Haberkorn, and A. Zimmer, The rate and mechanism of the gas-phase oxidation of hydroxyacetone, *Atmos. Environ.* 33, 1621-1629, doi: 10.1016/S1352-2310(98)00386-0, 1999.
- Röth, E.-P. and D.H. Ehhalt, A simple formulation of the  $\text{CH}_2\text{O}$  photolysis quantum yields, *Atmos. Chem. Phys.*, 15, 7195-7202, doi:10.5194/acp-15-7195-2015, doi:10.5194/acp-15-7195-2015, 2015.
- Sander, S. P., J. Abbott, J. R. Barker, J. B. Burkholder, R. R. Friedl, D. M. Golden, R. E. Huie, C. E. Kolb, M. J. Kurylo, G.K. Moortgat, V. L. Orkin and P. H. Wine, "Chemical Kinetics and Photochemical Data for Use in Atmospheric Studies, Evaluation No. 17," JPL Publication 10-6, Jet Propulsion Laboratory, Pasadena (2011). <http://ipldataeval.jpl.nasa.gov>.
- Volkamer, R., P. Spietz, J.P. Burrows, and U. Platt, High-resolution absorption cross-sections of glyoxal in the UV-vis and IR spectral ranges, *J. Photochem. Photobiol. A: Chem.* 172, 35-46, doi: 10.1016/j.jphotochem.2004.11.011, 2005.
- Yamamoto, S., and R.A. Back, R.A., The gas-phase photochemistry of oxalic acid, *J. Phys. Chem.*, 89,(4) 622-625, doi:10.1021/j100250a014, 1985.
- Zhu, L., D. Kellis, and C.-F. Ding, "Photolysis of glyoxal at 193, 248, 308, and 351 nm," *Chem. Phys. Lett.* 257, 487-491.